696 KSME International Journal, Vol. 11, No. 6, pp. 696~704, 1997

A Numerical Study of the Spatial Stability of Three-Dimensional Developing Plane Mixing Layer

Taewon Seo*

(*Received October 30, 1996*)

This paper is concerned with the hydrodynamic stability of the free shear layer. The concern of this study lies in obtaining solutions for the viscous spatially three-dimensional stability corresponding to the classical self-similar velocity profile of the free shear layer. In this study several techniques are applied to resolve the serious numerical complication introduced by the finite domain and parasitic contamination of the solution. As the spanwise wave number decreases, the neutral stability occurs at higher frequencies, β. The maximum amplification rate ($-\alpha_{imax}$) increases when spanwise wave number decreases. The decrease of $-\alpha_{imax}$ with γ at a fixed Reynolds number is quite linear with the exception of low spanwise wave number ($\gamma \leq 0.2$).

Key Words: Spatial Instability, Mixing Layer, Matching Method, Amplification Rate

Nomenclature

$C_{1,2,3}$	: The complex coefficients at $-\infty$
c	: The phase velocity
$D_{1,2,3}$	: The complex coefficients at ∞
$\tilde{p}$	: Large-scale coherent structure of pressure
$\hat{p}$	: Eigenfunction of pressure
R	: Velocity ratio
Re	: Reynolds number
t	: Time
$U_{\pm\infty}$	: Free stream velocities
$\tilde{u}, \tilde{v}, \tilde{w}$	: Large-scale coherent structures in the coordinate system
$\hat{u}, \hat{v}, \hat{w}$	: Eigenfunctions in the coordinate system
$\hat{u}'', \hat{v}'', \hat{w}''$	: Second derivative of Eigenfunctions with respective to η
$V^0_{-1,-2,-3}$	: Asymptotic solution at $-\infty$
$V^0_{1,2,3}$	: Asymptotic solution at ∞
α	: Complexwavenumber (Eigenvalues of linear stability problem)
β	: Frequency parameter
γ	: Spanwise wave number
δ	: Maximum slope thickness (1/2 of vorticity thickness)
η	: The stretched coordinate

* School of Mechanical Eng. Andong National Univ. 388 Songchon-Dong, Andong, Korea

1. Introduction

This paper is concerned with the hydrodynamic stability of the free shear layer. The development of mixing layer downstream of splitter plate is initially dominated by a linear stability mechanism. The schematic diagram of the flow for a spatially developing shear layer is sketched in Fig. 1. Intensive mixing occurs in the velocity gradient region between two free streams and such layers are often referred to as mixing layers. Shear layers are of practical importance in many fields where rapid transition to turbulence is desirable in order to prevent boundary layer separation or to promote rapid mixing.

A great deal of work has been done on hydrodynamic stability of parallel flows such as the free shear layer (Lin 1955; Betchov & Criminale 1967; Drazin & Reid 1982). Stability calculations for free shear layer by Lessen & Ko (1966) and Esch (1958) have in fact shown that for large Reynolds number the neutral curve approaches asymptotically the neutral value

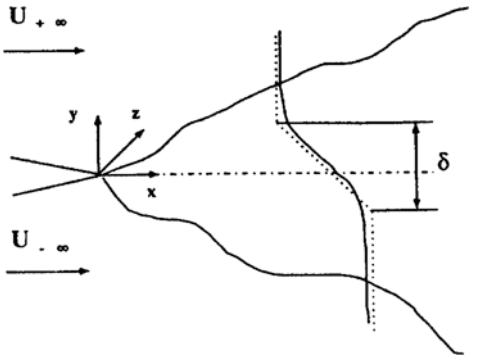

Fig. 1 Schematic diagram of a developing mixing layer

predicted by inviscid theory. The same result was obtained by Tatsumi & Kakutani (1958). Michalke (1965, 1968) has studied both two- and three-dimensional inviscid problem while Monkewitz & Huerre (1982) have provided inviscid solutions for different velocity profiles. Morris (1976) studied the stability of three axisymmetric jet profiles, and Lee (1988) investigated the eigenvalues and eigenfunctions of the stability for round jet. Recently, Seo (1995) formulated the linear stability problem for two-dimensional shear flow with a two-directional matching method.

In this study the linear stability of three-dimensional viscous shear layer is formulated, and the numerical investigation of the spatial stability of three-dimensional modes in a developing mixing layer is presented. A parametric study on the unstable mode characteristics to investigate the effects of the spanwise wave number and the Reynolds number is carried out.

2. Governing Equations

The problem is considered the three-dimensional shear flow of an incompressible viscous fluid and is assumed that the unperturbed flow has a sole mean velocity component parallel to the streamwise axis. The profile of the mean flow streamwise velocity component will be assumed to have the shape of a hyperbolic tangent function. This profile has been verified experimentally (Wygnanski & Fiedler 1970; Ho & Huang 1982) and used by many researchers (Kelly 1967; Monkewits & Huerre 1982; Nikitopoulos & Liu 1987). The local Reynolds number is defined as $Re=\frac{U\delta}{\upsilon}$, where δ is the local half maximum slope thickness of the shear layer.

For the spatial linear stability problem, we can assume

$$\tilde{u}(x,\eta,z,t)=\hat{u}(\eta)\,e^{i\alpha(x-ct)}\cos(\gamma z) \quad (1)$$

$$\tilde{v}(x,\eta,z,t)=\hat{v}(\eta)\,e^{i\alpha(x-ct)}\cos(\gamma z) \quad (2)$$

$$\tilde{p}(x,\eta,z,t)=\hat{p}(\eta)\,e^{i\alpha(x-ct)}\cos(\gamma z) \quad (3)$$

and

$$\tilde{w}(x,\eta,z,t)=\hat{w}(\eta)\,e^{i\alpha(x-ct)}\sin(\gamma z) \quad (4)$$

where β is the real frequency equal to αc. The imaginary part of the wave number $\alpha(\alpha=\alpha_r+i\alpha_i)$ determines the stability of the flow; the flow is stable if α_i has positive value, neutral if α_i is equal to zero, and unstable if α_i has a negative value.

When we substitute Eqs. (1) ~ (4) into the Navier-Stokes equations and linearize, we will get

$$i\alpha\hat{u}+\frac{d\hat{v}}{d\eta}+i\gamma\hat{w}=0 \quad (5)$$

$$i\alpha\left(U-\frac{\beta}{\alpha}\right)\hat{u}+\frac{dU}{d\eta}\hat{v}+i\alpha\hat{p}=-\frac{1}{Re}\left(\hat{u}''-\overline{\alpha^2}\hat{u}\right) \quad (6)$$

$$i\alpha\left(U-\frac{\beta}{\alpha}\right)\hat{v}+\frac{d\hat{p}}{d\eta}=-\frac{1}{Re}\left(\hat{v}''-\overline{\alpha^2}\hat{v}\right) \quad (7)$$

$$i\alpha\left(U-\frac{\beta}{\alpha}\right)\hat{w}+i\gamma\hat{p}=-\frac{1}{Re}\left(\hat{w}''-\overline{\alpha^2}\hat{w}\right) \quad (8)$$

where $\overline{\alpha^2}=\alpha^2+\gamma^2$.

If we are considering a two-dimensional disturbance ($\gamma=0$), these Eqs. (5) ~ (8) can be combined into one fourth-order ordinary differential equation for one unknown function which is the well known Orr-Sommerfeld equation. For the general three-dimensional disturbance the governing Eqs. (5) ~ (8) constitute a sixth-order system for the variables $\hat{u}$, $\hat{u}'$, $\hat{v}$, $\hat{p}$, $\hat{w}$, $\hat{w}'$ and the corresponding boundary conditions are;

$$at\ \eta\to\pm\infty\ ;\ \hat{u},\ \hat{v},\ \hat{p},\ \hat{w}\to 0 \quad (9)$$

For the spatial problem, the system of ordinary differential Eqs. (5) ~ (8) together with the boundary conditions given by Eq. (9) poses an

eigenvalue problem with α as the complex eigenvalue, $\hat{u}$, $\hat{v}$, $\hat{p}$ and $\hat{w}$ as eigenfunctions, and β, γ and Re as the real parameters.

If we define $D\hat{u} \equiv \frac{d\hat{u}}{d\eta}$, $D\hat{w} \equiv \frac{d\hat{w}}{d\eta}$ and the dependent variable vector $\vec{V}$ as

$$\vec{V} = \begin{pmatrix} \hat{u} \\ D\hat{u} \\ \hat{v} \\ \hat{p} \\ \hat{w} \\ D\hat{w} \end{pmatrix} \tag{10}$$

then the Eqs. (5) ~ (8) can be written as

$$\frac{d\vec{V}}{d\eta} = \boldsymbol{M}\vec{V} \tag{11}$$

where $\boldsymbol{M}$ is 6×6 matrix

$$\boldsymbol{M} = \begin{bmatrix} 0 & 1 & 0 & 0 & 0 & 0 \\ \Omega & 0 & Re\frac{dU}{d\eta} & i\alpha Re & 0 & 0 \\ -i\alpha & 0 & 0 & 0 & -i\gamma & 0 \\ 0 & -\frac{i\alpha}{Re} & -\frac{\Omega}{Re} & 0 & 0 & -\frac{i\gamma}{Re} \\ 0 & 0 & 0 & 0 & 0 & 1 \\ 0 & 0 & 0 & i\gamma Re & \Omega & 0 \end{bmatrix} \tag{12}$$

with $\Omega = \overline{\alpha^2} + i\alpha Re\,(U - \frac{\beta}{\alpha})$.

The eigenvalue problem posed by differential Eq. (11) with the boundary conditions will be solved numerically for the eigenvalue and eigenfunctions $\hat{u}$, $\hat{v}$, $\hat{p}$ and $\hat{w}$. In order to do this we need to look at the asymptotic behavior of the solutions at the boundaries of our infinite domain.

3. Asymptotic Solutions

In the numerical solution of eigenvalue problems on infinite intervals, a common method of proceeding is to replace the infinite interval by the appropriate finite interval. To get the asymptotic solutions, we solve the governing Eq. (11) in their limiting forms when $\eta \to \pm\infty$ where the mean velocity and its derivatives are equal to zero. The solution of the system which is now one of ordinary differential equation with constant coefficients is straight forward and the details can be found in Mack (1984).

At $\eta \to -\infty$ the asymptotic solution is

$$\begin{pmatrix} \hat{u} \\ D\hat{u} \\ \hat{v} \\ \hat{p} \\ \hat{w} \\ D\hat{w} \end{pmatrix} = C_1 \begin{pmatrix} \frac{i\alpha}{\bar{\alpha}} \\ i\alpha \\ 1 \\ -i\alpha(U_{-\infty} - \beta/\alpha) \\ \frac{i\gamma}{\bar{\alpha}} \\ i\gamma \end{pmatrix} e^{\alpha\eta} + C_2 \begin{pmatrix} \frac{i\alpha x}{\alpha^2} \\ \frac{i\alpha x^2}{\alpha^2} \\ 1 \\ 0 \\ \frac{i\gamma x}{\alpha^2} \\ \frac{i\gamma x^2}{\alpha^2} \end{pmatrix} e^{ix\eta} + C_3 \begin{pmatrix} -\frac{\gamma}{\bar{\alpha}} \\ -\frac{\gamma x}{\bar{\alpha}} \\ 0 \\ 0 \\ \frac{\alpha}{\bar{\alpha}} \\ \frac{\alpha x}{\bar{\alpha}} \end{pmatrix} e^{\kappa\eta} \tag{13}$$

or

$$\boldsymbol{V}_{-}^{0} = C_1\ \boldsymbol{V}_{-1}^{0} + C_2\ \boldsymbol{V}_{-2}^{0} + C_3\ \boldsymbol{V}_{-3}^{0} \tag{14}$$

and at $\eta \to \infty$ the asymptotic solution is

$$\begin{pmatrix} \hat{u} \\ D\hat{u} \\ \hat{v} \\ \hat{p} \\ \hat{w} \\ D\hat{w} \end{pmatrix} = D_1 \begin{pmatrix} -\frac{i\alpha}{\bar{\alpha}} \\ i\alpha \\ 1 \\ i\alpha(U_{-\infty} - \beta/\alpha) \\ -\frac{i\gamma}{\bar{\alpha}} \\ i\gamma \end{pmatrix} e^{-\alpha\eta} + D_2 \begin{pmatrix} -\frac{i\alpha x}{\alpha^2} \\ \frac{i\alpha x^2}{\alpha^2} \\ 1 \\ 0 \\ -\frac{i\gamma x}{\alpha^2} \\ \frac{i\gamma x^2}{\alpha^2} \end{pmatrix} e^{-ix\eta}$$

$$+D_3\begin{pmatrix} -\frac{\gamma}{\bar{\alpha}} \\ -\frac{\gamma\chi}{\bar{\alpha}} \\ 0 \\ 0 \\ \frac{\alpha}{\bar{\alpha}} \\ -\frac{\alpha\chi}{\bar{\alpha}} \end{pmatrix} e^{-\kappa\eta} \tag{15}$$

or

$$V_+^0 = D_1\ V_1^0 + D_2\ V_2^0 + D_3\ V_3^0 \tag{16}$$

where $\chi = \sqrt{\bar{\alpha}^2 + i\alpha Re\,(U_{\pm\infty} - \beta/\alpha)}$, V_{+1}^0 is the inviscid solution, and $V_{\pm 2}^0$, $V_{\pm 3}^0$ are the primary and secondary viscous solutions respectively. The coefficients C_1, C_2, C_3, D_1, D_3 and D_3 are complex constants to be determined. These asymptotic solutions will be used as initial conditions to solve the system of Eq. (11).

4. Numerical Methods

The numerical method used for the eigenvalue problem in hand is a classical shooting method. We have used several techniques to resolve the serious numerical complications introduced by the infinite domain and parasitic contamination of the solution. The general process requires that the appropriate system of Eq. (11) is integrated from $-\eta_{-\infty}$ to 0 and from η_∞ to 0, and the two computed solutions are matched at a matching point as shown in Fig. 2.Matching can be achieved only for the correct value of α and thus the matching condition becomes the dispersion relation which is solved iteratively by a numerical root finding method.

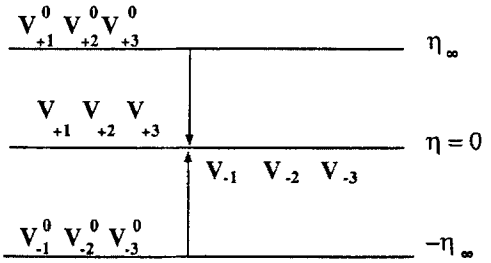

Fig. 2 A diagram for two-directional integration method at a matching point

A Runge-Kutta-Fehlberg method is used to integrate the ordinary differential equations. This scheme controls the step size by keeping an estimate of the local error below the user specified tolerance (in this study 1×10^{-08}). The estimate of local error is obtained by comparing the two values evaluated by a fourth-order method and fifth-order method.

For correct eigenvalue, the general solution at the matching point ($\eta_m=0$) must satisfy

$$\begin{aligned} \boldsymbol{V}_-(\eta_m) &= C_1\boldsymbol{V}_{-1}(\eta_m) + C_2\boldsymbol{V}_{-2}(\eta_m) \\ &\quad + C_3\boldsymbol{V}_{-3}(\eta_m) \\ &= \boldsymbol{V}_+(\eta_m) = D_1\boldsymbol{V}_{+1}(\eta_m) + D_2\boldsymbol{V}_{+2} \\ &\quad (\eta_m) + D_3\boldsymbol{V}_{+3}(\eta_m) \end{aligned} \tag{17}$$

Rewriting Eq. (17) in matrix form, we have

$$\boldsymbol{GC} = [\,\boldsymbol{V}_{-1}\ \boldsymbol{V}_{-2}\ \boldsymbol{V}_{-3}\ \boldsymbol{V}_{+1}\ \boldsymbol{V}_{+2}\ \boldsymbol{V}_{+3}] \begin{pmatrix} C_1 \\ C_2 \\ C_3 \\ D_1 \\ D_2 \\ D_3 \end{pmatrix} = 0 \tag{18}$$

This matching condition is satisfied if the determinant of matrix $\boldsymbol{G}$ is equal to zero;

$$\Delta(\alpha, \beta, \gamma, Re) \equiv det\ \boldsymbol{G} = 0 \tag{19}$$

This constitutes the dispersion relation and the eigenvalue is calculated from it using the iterative technique.

The following iterative technique is used to find the eigenvalue. The numerical integrations are carried out once with an initial estimated value α_1, and a second time with a value, α_2, which is obtained by slightly changing α_1. If Δ_1 or Δ_2 is not less than a prescribed tolerance (e.g. 1×10^{-08}), the Lagrange interpolation scheme is used in order to find a new estimate α_{n+1};

$$\alpha_{n+1} = \sum_{i=1}^{n}\left[\prod_{j=1, i\neq j}^{n} \frac{-\Delta_j}{\Delta_i - \Delta_j}\right]\alpha_i \quad \text{for } n\geq 2 \tag{20}$$

The simple and mathematically exact superposition method does not work when Reynolds number is large (larger than 90 in this study). The matrix $\boldsymbol{G}$ in Eq. (18) will poorly conditioned at the matching point and consequently the convergence criteria will never be met within a desired accuracy. In other words, if Reynolds number is

higher, the three independent solutions will lose their linear independence because of contaminating error particularly in the viscous region of the mixing layer. Therefore, the eigenvalue and eigenfunctions obtained by the simple superposition method will not be accurate at all. An orthonormalization method is used in order to keep the independence of these sets of solutions.

The orthonormalization method was developed by Conte (1966) and Davey (1973). To briefly explain the orthonormalization method, first apply the Gram-Schmidt recursion formulas for orthonormalizing a set of vectors $[V_{-1}, V_{-2}, V_{-3}, V_1, V_2, V_3]$ as $[U_1, U_2, U_3, U_4, U_5, U_6]$;

$$U_1=\frac{V_1}{\|V_1\|}$$

$$U_k=V_k-\sum_{i=1}^{k-1}[(V_k,\ U_i)\,U_i/(\|(V_k,\ U_i)\,U_i\|)]\quad k=2,\cdots,6$$

This method has been successfully applied by Morris (1976), Lee (1988) and Seo (1995).

5. Numerical Results and Discussion

The computed three-dimensional spatial amplification rates for hyperbolic tangent profile with velocity ratio R=0.31 are plotted versus nondimensional frequency in Fig. 3 for several values of the spanwise wave numbers for Reynolds number equal to 1,000.The hyperbolic tangent profile is defined as $U=1-Rtanh(\eta)$. As long as the amplification rate $-\alpha_i$ is positive, the large-scale disturbances are amplified. When α_i becomes zero, the disturbance is neither amplified nor damped and is neutrally stable. For higher frequencies beyond the neutral value the shear layer becomes stable in Fig. 3 and the disturbance is damped. From Fig. 3 we see that the neutral stability point moves to lower frequencies as the spanwise wave number increased because the smaller scales are more dissipative.

The calculated maximum amplification rates $-\alpha_{imax}$ are shown in Fig. 4 as a function of Reynolds number for various spanwise wave number γ. As Reynolds number increased, the maximum growth rate increases monotonically and asymptotically by approaching the inviscid limit. The growth rate is of course always the largest in the two-dimensional case ($\gamma=0$) which is the lower limit of γ. For any given spanwise wave number, there is a critical Reynolds number below which the three-dimensional disturbance is

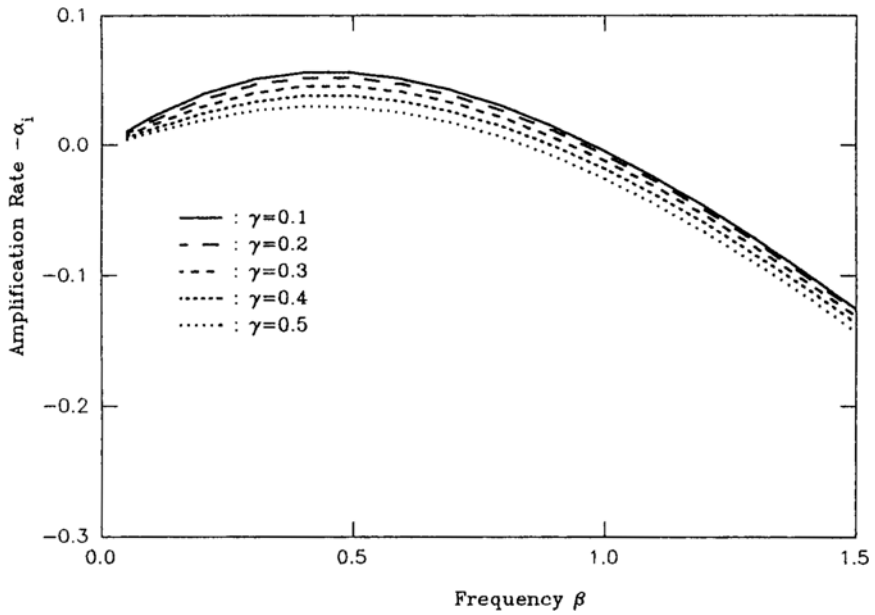

Fig. 3 Amplification rates $-\alpha_i$ versus nondimensional frequency β with various spanwise wave number γ and Re=1,000

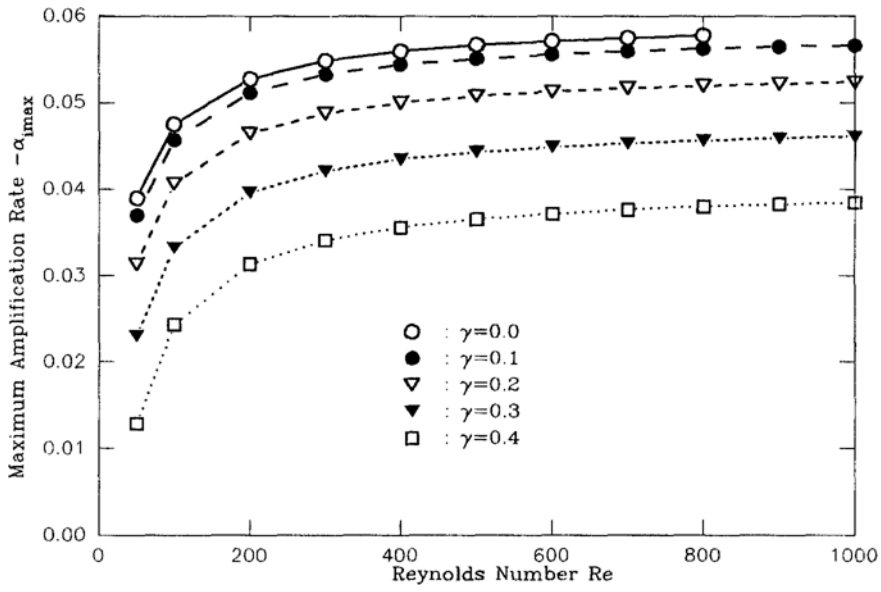

(a)

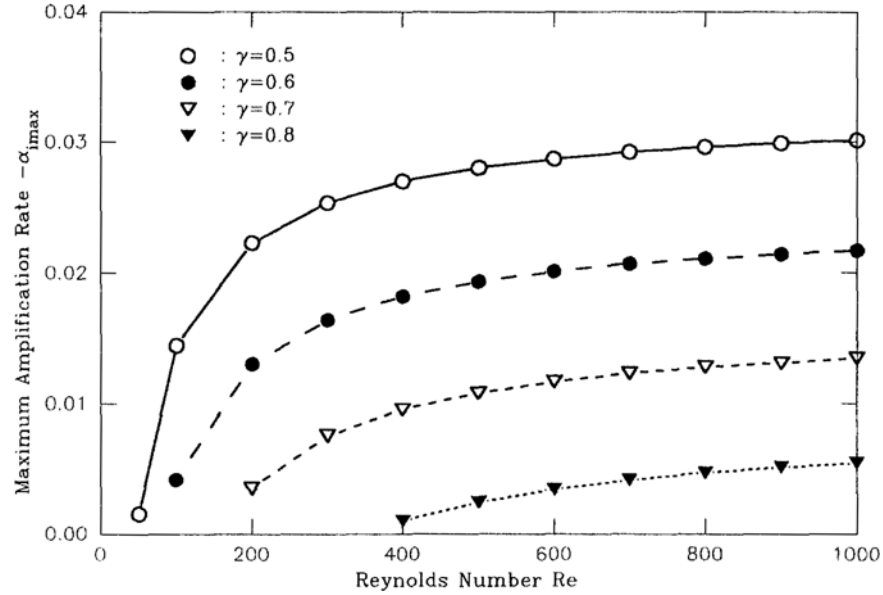

(b)

Fig. 4 The maximum amplification rates $-\alpha_{imax}$ versus Reynolds number for various spanwise wave number γ

damped for all frequencies. As it can be deduced from Fig. 4, the critical Reynolds number increases with increasing γ. For values of spanwise wave number γ larger than approximately 0.5, this critical Reynolds number increases considerably. For instance, the critical Reynolds number for $\gamma=0.8$ is approximately 350. For two-dimensional case, we have calculated the critical Reynolds number to be approximately 12.5 as shown in Fig. 5 where the neutral stability curve is shown in frequency versus Reynolds number space. Below this value, all

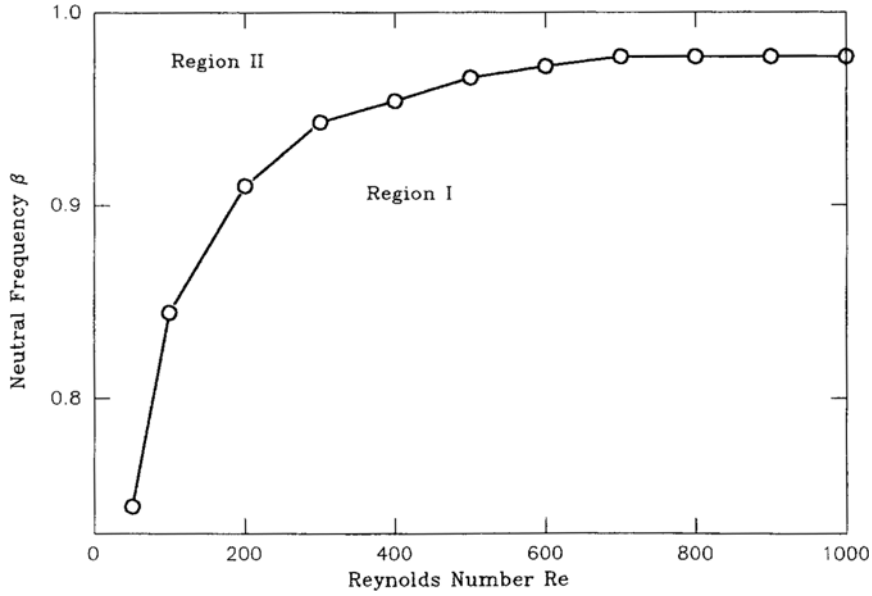

Fig. 5 The neutral stability curve for two-dimensional disturbances

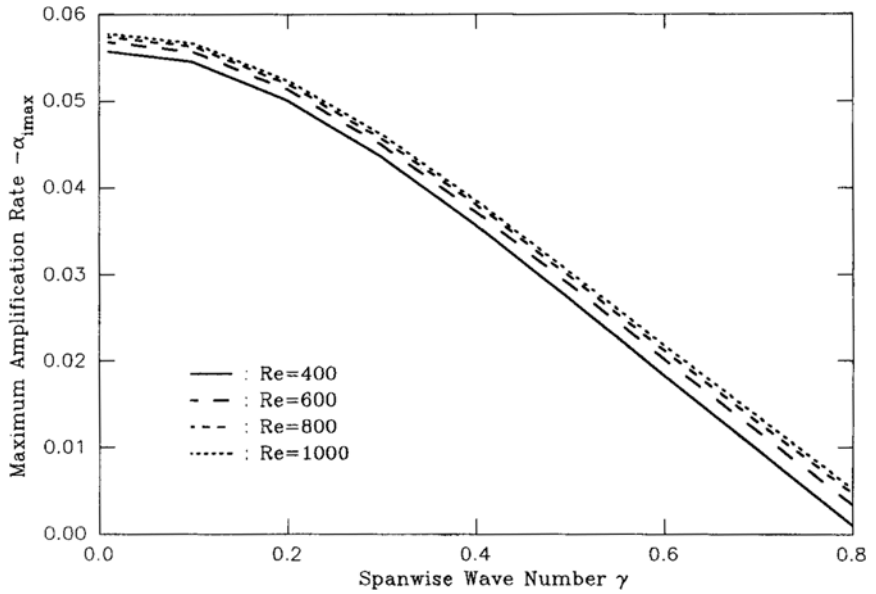

Fig. 6 The maximum amplification rates $-\alpha_{imax}$ versus spanwise wave number γ for several Reynolds numbers

disturbances are damped. In region I the two-dimensional disturbance is unstable and stable in region II. Of course, it is well known that at very low Reynolds numbers the parallel mean flow assumption may not be exactly valid and therefore the critical Reynolds number calculated here may not be exactly correct.

The variation of the maximum amplification rate with spanwise wave number γ for several Reynolds numbers is shown in Fig. 6. The maximum amplification rate increases when spanwise wave number γ decreases. The decrease of $-\alpha_{imax}$ with γ at a fixed Reynolds number is quite linear with the exception of low spanwise wave number

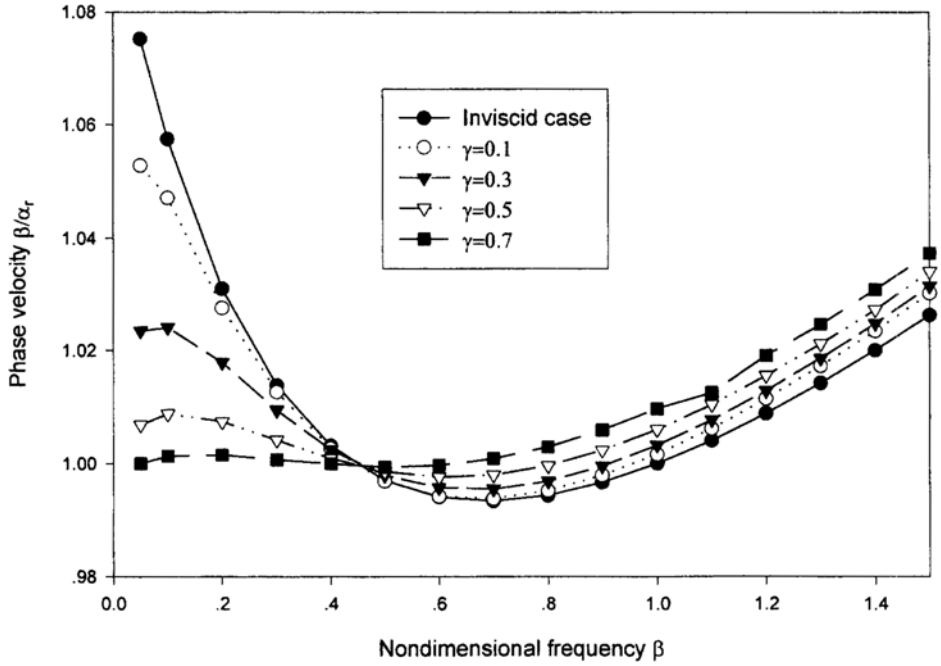

Fig. 7 Phase velocity for various spanwise wave numbers.

($\gamma \leq 0.2$). This is in good agreement with the inviscid results of Michalke (1969). Three-dimensional wave modes of long wavelength are more likely to occur in a shear layer if their amplification rates can be boosted through combined forcing and interaction with other modes. It is understood that the amplification rate shown here result from interaction with the mean flow alone.

The phase velocities as a function of β and γ for the three-dimensional mode are shown in Fig. 7. The phase velocity gradually approaches the inviscid solution as γ decreases. According to the result, the phase velocity decreases with frequency at low frequencies and increases at high frequencies.

6. Conclusions

In this work, the viscous linear stability of the three-dimensional, homogeneous shear layer is analyzed. The mean flow profile is prescribed by the hyperbolic tangent profile. The unstable mode characteristics are interpreted in terms of two independent parameters: Reynolds number and the spanwise wave number. The computed results are summarized as follows;

(1) The growth rate for $\gamma \neq 0$ are always smaller than for $\gamma = 0$ and the three-dimensional disturbances are less unstable than two-dimensional disturbances.

(2) The neutral stability occurs at higher frequencies, as spanwise wave number decreases.

(3) As Reynolds number increased, the maximum growth rate increases monotonically and asymptotically approaching the inviscid limit.

(4) The decrease of $-\alpha_{imax}$ with γ at a fixed Reynolds number is quite linear with the exception of low spanwise wave number ($\gamma \leq 0.2$).

References

Betchov, R. and Criminal, W. O., 1967 *Stability of Parallel Flows*, First edn, Academic Press.

Conte, S. D., 1966, "The Numerical Solution of Linear Boundary Value Problem," *SIMA Review* Vol. 8, pp. 309~321.

Davey, A., 1973, "A Simple Numerical Method for Solving Orr-Sommerfeld Problems," *Quart. J. Mech. Appl. Math.*, Vol. 26, pp. 401~411.

Drazin, P. G. and Reid, W. H., 1981, *Hydrodynamic Stability*, First edn, Cambridge Univ. Press

Esch, R. E., 1957, "The Instability of Shear Layer Between Two Parallel Stream," *J. Fluid Mech.*, Vol. 3, pp. 289~303.

Ho, C. M. and Huang, L. S., 1982, "Subharmonics and Vortex Merging in Mixing Layers," *J. Fluid Mech.*, Vol. 119, pp. 443~473.

Kelly, R. E., 1967, "On the Stability of an Inviscid Shear Layer which is Periodic in Space and Time," *J. Fluid Mech.*, Vol. 27, pp. 657~689.

Lee, S. S., 1988, "Multiple Coherent Interaction in a Developing Round Jet," Ph. D. Thesis, Brown Univ.

Lessen, M. and Ko, S. H., 1966, "Viscous Instability of an Incompressible Fluid Half-Jet Flow," *Phys. Fluid* 9, pp. 1179~1183.

Lin, C. C., 1955, *The Theory of Hydrodynamic Stability*, Cambridge Univ. Press.

Mack, L. M., 1984, "Boundary-Layer Laminar Stability Theory," *In Special Course on Stability and Transition of Laminar Flow*, AGARD Rep. R-709, 3.1~3.81.

Michalke, A., 1965, "On Spatially Growing Disturbances in an Inviscid Shear Layer," *J. Fluid Mech.*, Vol. 23, pp. 521~544.

Michalke, A., 1969, "A Note on Spatially Growing Three-Dimensional Disturbance in a Free Shear Layer," *J. Fluid Mech.*, Vol. 38, pp. 765~767.

Monkewitz, P. A. and Huerre, P., 1982, "Influence of the Velocity Ratio on the Spatial Instability of Mixing Layers," *Phys. Fluid* Vol. 25, pp. 1137~1143.

Morris, P. J., 1976, "The Spatial Viscous Instability of Axisymmetric Jets," *J. Fluid Mech.*, Vol. 77, 511~529.

Nikitopoulos, D. E. and Liu, J. T. C., 1987, "Nonlinear Binary-mode Interactions in a Developing Mixing Layers," *J. Fluid Mech.*, Vol. 179, pp. 345~370.

Seo, T. W., 1995, "The Spatial Viscous Instability of a Two-Dimensional Developing Mixing Layer," *KSME Journal*, Vol. 9, No. 1, pp. 14~18.

Tatsumi, T. and Kakutani, T., 1958, "The Stability of Two-Dimensional Laminar Jet," *J. Fluid Mech.*, Vol. 4, pp. 216~275.

Wygnanski, I. and Fiedler, H. E., 1970, "The Two-dimensional Mixing Region," *J. Fluid Mech.*, Vol. 41, pp. 327~361.